Minimization of Iron Losses of Permanent Magnet Synchronous Machines

Chunting Chris Mi, *Senior Member, IEEE*, Gordon R. Slemon, *Life Fellow, IEEE*, and Richard Bonert, *Member, IEEE*

***Abstract*—In permanent magnet (PM) synchronous machines, iron losses form a larger portion of the total losses than in induction machines. This is partly due to the elimination of significant rotor loss in PM machines and partly due to the nonsinusoidal flux density waveforms in the stator core of PM machines. Therefore, minimization of iron losses is of particular importance in PM motor design. This paper considers the minimizing of iron losses of PM synchronous machines through the proper design of magnets and slots, and through the choice of the number of poles. Both time-stepped finite element method (FEM) and the iron loss model from a previous study are used in this paper to draw the conclusions.**

***Index Terms*—Eddy currents, hysteresis, magnetic losses, permanent magnet machines, synchronous machines.**

I. Introduction

ELECTRIC motor-driven equipment utilizes approximately 58% of the consumed electrical energy [1]. Of this electrical motor usage, 93% is consumed by induction motors with power ratings of 5.1 hp and greater, 5% is consumed by induction motors with power ratings of 5 hp or less. DC motors and synchronous motors consume only 2% of the total electrical motor usage [2]. In the past decades, the cost of electrical power increased dramatically [3]. This trend has forced many manufacturers to address the problem of improving the efficiency of electrical motors.

Since induction motors consume most of the electrical motor usage, the focus has been placed on the optimization of induction machines. However, induction motors have their own limitations, e.g., the rotor loss always exists. This has lead to a search for alternative approaches. One important approach among them is to use variable speed permanent magnet (PM) synchronous motors.

With proper design, a PM machine will generally have higher energy efficiency than any other type of rotating machines of equivalent power output. This is due to the elimination of field ohmic loss as compared to DC excited machines, or due to the elimination of the rotor loss as compared to induction motors. PM machines not only have the advantage of higher efficiency, but also have many other advantages such as less volume and weight, higher power factor and easier controllability.

Manuscript received June 24, 2002; revised September 26, 2003. Paper no. TEC-00145-2002.

C. Mi is with the Department of Electrical and Computer Engineering, University of Michigan, Dearborn, MI 48128-1491 USA (e-mail: chrismi@umich.edu).

G. R. Slemon and R. Bonert are with the Department of Electrical and Computer Engineering, University of Toronto, Toronto, ON M5S 3G4, Canada (e-mail: g.slemon@utoronto.ca; r.bonert@utoronto.ca).

Digital Object Identifier 10.1109/TEC.2004.832091

There was very little interest in PM machines for drive systems two decades ago. It was only when new rare-earth PM materials with their high energy products and relatively low cost became available that industry recognized PM machines were not just low power devices of minimal commercial importance [4]. With the technology advancements and cost reductions in modern rare-earth PM materials and power electronics, it is now possible to use motors in many applications such as pumps, fans, compressors, electrical vehicles and traction drives, where the higher initial cost can be rapidly paid back by energy savings often within a year [5].

The overall optimization of a PM synchronous motor requires a balance between the manufacturing cost, efficiency, power factor and torque capability. In most cases, these parameters conflict with each other and compromises have to be made [6]–[9]. The losses of a PM synchronous motor can be decomposed into four components, namely stator winding loss, iron loss, mechanical loss and stray load loss. Iron losses of PM machines form larger portion of the total losses than that in induction machines. Therefore, prediction of iron losses of PM machines remains one of the most interested topics of PM motor designers [10]–[13]. Design considerations have been proposed for different categories of PM motors [14]–[18]. Minimization of iron losses from the control point of view was also studied [19].

In this paper, some design approaches are proposed to minimize the iron losses of PM synchronous motors through proper design of magnets and slots, and through the choice of the number of poles.

II. Evaluation of Iron Losses of PM Machines

The iron losses in electrical machines have usually been evaluated by assuming that the flux density in the core material is sinusoidal. The predicted losses in this procedure are usually much less than the measured iron losses [20]. A more reliable method is to evaluate the iron losses using finite element method (FEM).

For eddy current, it is convenient to represent the average loss density as a function of the time rate of change of the vector flux density [21]–[23]. Then both eddy current loss and hybrid loss can be evaluated using time-stepped FEM [23]

$$P_e = \frac{p}{2}\sum_{m=1}^{M} A_m l_{fe} \frac{2k_e}{T} 2 \int_0^{\frac{T}{2}} \left(\frac{d\mathbf{B}}{dt}\right)^2 dt = 2pNk_e l_{fe} f^2$$

$$\times \sum_{m=1}^{M} \left\{ A_m \left[\sum_{n=1}^{N} (B_{mx,n} - B_{mx,n-1})^2 + \sum_{n=1}^{N} (B_{my,n} - B_{my,n-1})^2 \right] \right\} \quad (1)$$

$$P_h = 2\pi k_h l_{fe} f \sum_{m=1}^{M} \left[A_m B_{m,\max}^{\beta} \right] \quad (2)$$

where $P_{\rm e}$ is eddy current loss, $P_{\rm h}$ is hysteresis loss, p is the number of poles, N is the number of steps used in time-stepped FEM, $l_{\rm fe}$ is the effective length of core, $k_{\rm e}$ and $k_{\rm h}$ are the eddy loss constant and hysteresis loss constant of the core material respectively, f is the frequency, $A_{\rm m}$ is area of element m, $B_{\rm mx,n}$ and $B_{\rm my,n}$ are the radial and circumferential component of the flux density of element m at time step n of the time-stepped FEM respectively, $B_{\rm m,max}$ is the maximum flux density of element m during the time-stepped FEM analysis of the PM machine, T is the period, and M is the total number of elements.

Although the FEM gives highly accurate loss predictions, it consumes enormous time during the iteration of the design. A simplified iron loss model was developed by the authors [23]. For a PM motor with rectangular edged magnets, tooth and yoke flux density waveforms are approximately trapezoidal. The eddy current loss in the teeth and yoke of a PM machine can be expressed as follows [23]

$$P_{et} = \frac{4m}{\pi^2} q k_q k_c k_e (\omega_s B_t)^2 V_t \quad (3)$$

$$P_{ey} = \frac{1}{\alpha} \frac{8}{\pi^2} k_e k_r \omega_s^2 B_y^2 V_y \quad (4)$$

where α is the fractional magnet coverage, ω_s is the angular frequency, $P_{\rm et}$ and $P_{\rm ey}$ are tooth and yoke eddy current loss respectively, m is number of phases, q is the number of slots per pole per phase, $k_{\rm q}$ is a correction factor for geometrical dimensions of the machine, $k_{\rm c}$ is a correction factor for the eddy loss induced by the circumferential component of tooth flux density, $k_{\rm r}$ is a correction factor for the eddy loss induced by the radial component of yoke flux density, $B_{\rm t}$ and $B_{\rm y}$ are plateaus of tooth and yoke flux density respectively, $V_{\rm t}$ and $V_{\rm y}$ are tooth and yoke volume per pole respectively. $k_{\rm r}$ and $k_{\rm c}$ is usually in the rage of 1.05 to 1.15, $k_{\rm q}$ is usually in the range of 0.9 to 1.1. Refer to [23] for detailed calculation of these factors.

Tooth and yoke hysteresis loss can be expressed as

$$P_{ht} = k_h \omega_s B_t^{\beta} \quad (5)$$

$$P_{hy} = k_h \omega_s B_y^{\beta}. \quad (6)$$

It can be seen from (3)–(6) that tooth eddy current loss is proportional to the number of slots per pole per phase and yoke eddy current loss is inversely proportional to magnet coverage. The hysteresis loss is proportional to the plateau of the flux density.

III. Experimental Motor

For experimental purpose, a PM motor was constructed using the frame of a 3.73 kW, 4-pole, 60 Hz, 36-slots induction motor manufactured by General Electric Canada Inc. The sizes of the induction machine are shown in Table I. The efficiency of the original induction motor was 78.9% and power factor was 0.78. The preliminary design of the PM motor was designed using the same stator core and winding of the induction motor.

TABLE I
Dimensions and Parameters of Experimental Motor

Name	Value	Name	Value
Inner radius of stator (mm)	58.5	Stator length (mm)	88.9
Outer radius of stator (mm))	95	Tooth width (mm)	5.3
Thickness of magnets (mm)	6.3	Yoke depth (mm)	17.4
Tooth flux density (T)	1.2398	Tooth height (mm)	19.1
Yoke flux density (T)	1.2827	Magnet coverage	0.667
Tooth volume (m^3)	0.000380	Slot opening (mm)	3
Yoke volume (m^3)	0.000838	Airgap length (mm)	2

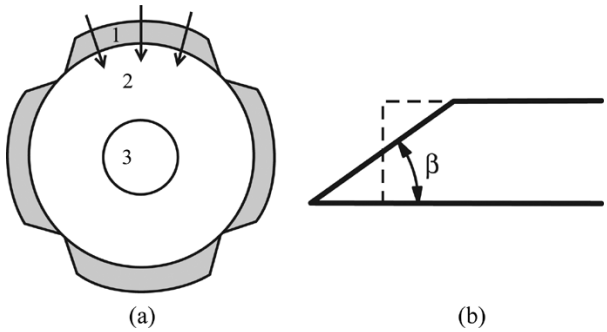

Fig. 1. Beveling of magnets. (a) A PM rotor using beveled magnets; (b) Beveling of the magnet edges. The usual practice is to design rectangular edged magnets as shown with the dashed outline in figure (b). The solid outline in figure (b) shows a bevel of β degrees of the magnet edge. Where, 1-magnet, 2-rotor core, 3-shaft and the arrow indicates the direction of magnetization.

IV. Design of Magnets

Equation (3) and (4) were developed for rectangular edged magnets. With rectangular edged magnets, the tooth and yoke flux density has roughly a trapezoidal waveform with the slope and plateau not appreciably affected by the angular width of the magnets. A change in the shape of the magnets will affect the slope of the flux density waveform and therefore affect the eddy current loss.

A. Beveling of Magnets

Beveling of the magnet edges can reduce the slope of the tooth flux waveform and reduce the eddy loss. In order to test this statement, FEM analyses were performed on the experimental 4-pole PM motor with varying magnet edges as shown in Fig. 1.

In order to obtain consistent results, the magnet volume was kept constant when beveling the magnet edge. Table II shows the calculated iron losses of the motor by FEM for different magnet edges.

It can be seen from Table II that when the bevel of magnet edge is increased, the tooth eddy loss decreases. The tooth eddy current loss of a beveled PM motor is reduced by 9.5% compared to that of a nonbeveled motor while other components of iron losses were nearly constant over the range of magnet edge beveling. The total iron losses are reduced 3.8% while the total airgap flux is kept nearly constant (Fig. 2).

TABLE II
TOOTH EDDY CURRENT LOSS VS. MAGNET EDGE BEVELING AT 120 Hz

	90	75	63	51	39	27
Tooth eddy current loss (W)	17.3	17.2	17.1	16.9	16.5	15.7
Tooth hysteresis loss (W)	10.9	10.8	10.8	10.5	10.8	10.8
Yoke eddy current loss (W)	18.1	18.1	18.1	18.0	18.0	17.8
Yoke hysteresis loss (W)	22.4	22.4	22.4	22.4	22.4	22.6
Total iron loss (W)	68.7	68.7	68.5	67.8	67.5	66.1
Airgap flux (x10^{-3} Wb)	5.2	5.20	5.20	5.20	5.21	5.22
Tooth eddy loss reduction (%)	-	0.3	1.0	2.4	4.7	9.5
Reduction of iron loss (%)	-	0.0	0.3	1.3	1.8	3.8

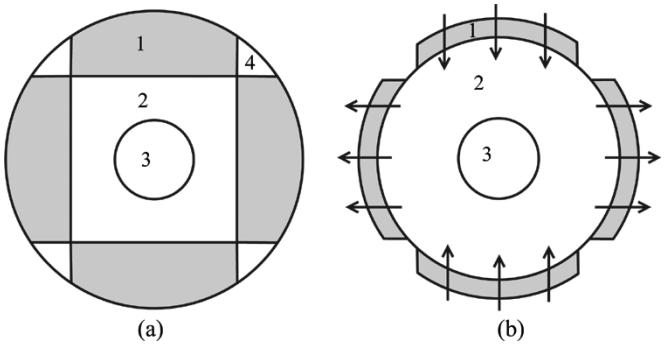

Fig. 2. Curved and parallel magnetized magnets in PM synchronous machines, where 1-magnet, 2-rotor core, 3-shaft, 4-nonmagnetic material. (a) A PM rotor using curved magnets; (b) a PM rotor with parallel magnetized magnets.

B. Shaping of Magnets

Based on the above observations, similar but alternative approaches can be employed to achieve the same effect as magnet edge beveling.

One method is to use curved magnets with the thickest in the center and the thinnest at the two ends as shown in Fig. 2(a). The curved magnets will improve the curvature of the flux waveforms. Therefore, the eddy current loss can be reduced. The drawback of this method is that the manufacturing cost of the magnets will be increased.

Another approach is to parallel magnetize the magnets or gradient magnetize the magnets with the flux increasing from the two ends to the middle of the magnets as shown in Fig. 2(b). The drawback of this approach is that the magnets are not fully utilized.

C. Magnet Width and Magnet Coverage

In [23], it was shown that changing magnet width over a wide range does not change the achieved maximum flux density in the teeth, nor does it change the slope of the tooth flux waveforms. However, when the space between the two adjacent magnets is less than one slot pitch, the slope of tooth flux density begins to increase. Especially when magnet coverage approaches 1.0, the slope of the tooth flux density is dramatically increased thus the tooth eddy current losses are significantly increased. At the other extreme, when the magnet width is less than one slot pitch, the tooth flux density reaches a plateau but its value is lower, although the slope of the flux density waveform is still the same.

Therefore, for a PM motor, in order to limit the tooth eddy current loss, the optimum magnet coverage is

$$\frac{1}{mq} \le \alpha \le \frac{mq-1}{mq}. \tag{7}$$

Since yoke eddy current loss is inversely proportional to magnet coverage as shown in (4), the magnet coverage should be large enough in order to minimize yoke eddy current loss. The achieved total airgap flux linkage is proportional to the width of the plateau of tooth flux density. Therefore, the magnet width must be sufficient to provide desired airgap flux linkage.

Magnet width also has significant effects on cogging torque of PM motors [24]. The optimum magnet coverage to achieve the least cogging torque is

$$\alpha = \frac{(n+0.14)\lambda}{\tau} = \frac{n+0.14}{mq} \tag{8}$$

where n is any integer which satisfies $\alpha < 1$, τ is the pole pitch, and λ is the slot pitch.

Combining (7) and (8), the optimum magnet coverage can be obtained. For example, for a PM motor with two slots per pole per phase ($m = 3$, $q = 2$), the magnet coverage that satisfy (7) and (8) is $\alpha = 0.523$ or $\alpha = 0.69$. In order to minimize yoke eddy current loss and maximize flux linkage in the motor, the optimal magnet coverage should be $\alpha = 0.693$.

V. DESIGN OF SLOTS

A. Number of Slots

For a given supply frequency, tooth eddy current loss is proportional to the number of slots per pole-phase. Hence, it is beneficial to use fewer but wider teeth. The minimum number of integer slots is one slot per pole per phase.

For a reasonably good approximation to a sinusoidal distribution of induced emf, there should be at least two slots per pole-phase [25]. For small PM motors, the use of two slots per pole-phase is practical. For large electrical machines, the slots per pole-phase should be as few as possible.

B. Slot Closure

By increasing slot closure, the maximum airgap flux density can be increased for the same amount of magnet used. The flux distribution of an 8-pole PM motor with different slot closure is shown in Fig. 3.

Small slot openings are widely used in most small motor designs. Although reducing slot openings does not reduce the stator iron losses, it increases the flux, the developed torque and therefore the percentage eddy loss.

Totally closed slots, as shown in Fig. 3(a), will increase leakage flux in the shoes of the teeth. This leakage flux does not contribute to the developed torque but increases the iron loss in that area. Therefore, totally enclosed slots are not recommended.

VI. CHOICE OF NUMBER OF POLES

Variable speed drives are free from the constraint on the number of poles imposed on ac motors operated at fixed fre-

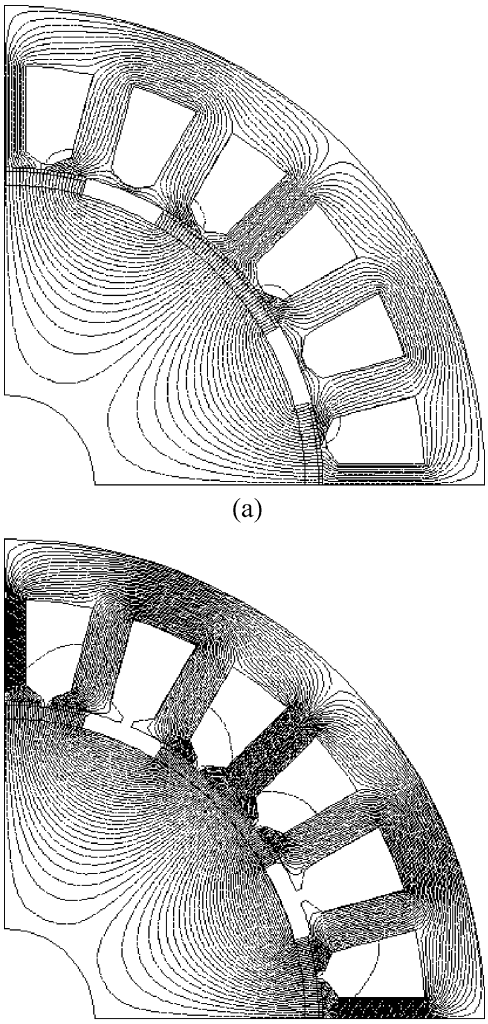

Fig. 3. Flux distribution with different slot closure. (a). Totally enclosed slots; (b). partly closed slots. In the case of totally closed slots, the magnetic flux of the magnet passes the closure from one pole to the adjacent pole.

quency. The inverter can be operated at variable frequencies, currents, and voltages. This allows the number of poles to be selected freely to achieve the best motor design. By increasing the number of poles, the length of the end turn windings is reduced and thus the copper usage can be reduced and the stator copper loss reduced. The thickness of the stator yoke is also reduced and therefore the usage of core material for the yoke is reduced. More power output or torque can be achieved by using more poles for the same frame due to the reduction of yoke thickness and increase in the inner radius of the stator.

Since the operating frequency increases proportionally to the number of poles in order to achieve the desired speed, both eddy current loss and hysteresis loss increase despite the fact that the mass of the stator core material is reduced.

In order to have a reasonable comparison base, the following analysis assumes a given frame and speed. This assumption results in a fixed machine core length and a constant friction and windage loss. Further, the copper weight and stator current are assumed constant, e.g., the copper loss is assumed roughly constant.

TABLE III
IRON LOSS AS A FUNCTION OF THE NUMBER OF POLES

Number of poles	2	4	6	12
Operating frequency (Hz)	30	60	90	180
Tooth eddy current loss (W)	8.7	17.3	26.0	52.0
Yoke eddy current loss (W)	8.6	18.1	27.5	55.9
Tooth hysteresis loss (W)	5.5	10.9	16.3	32.7
Yoke hysteresis loss (W)	21.3	22.4	22.7	23.1
Total iron losses (W)	44.0	68.7	92.6	163.7

A. Iron Losses and Number of Poles

Total number of slots is usually limited by the frame size. When the total number of slots is fixed, the number of slots per pole-phase is inversely proportional to the number of poles. The tooth eddy current loss and hysteresis loss can be written as functions of speed. From (3), considering that $\omega_s = (2\pi n/60) * (p/2)$, the tooth eddy current loss can be expressed as

$$P_{et} = \frac{pS}{900} k_q k_c k_e B_t^2 n^2 V_t \tag{9}$$

and from (5), the tooth hysteresis loss can be expressed as

$$P_{ht} = \frac{\pi np}{60} k_h B_t^{\beta} V_t \tag{10}$$

where $S = mpq$ is the total slots of the stator.

Therefore, both tooth eddy current losses and tooth hysteresis losses are proportional to number of poles.

Yoke volume can be expressed as a function of number of poles

$$V_y = \left[\pi r_j^2 - \pi\left(r_j - \frac{2}{p} d_{y2}\right)^2\right] l_{fe} = \frac{4\pi d_{y2}}{p}\left(r_j - \frac{d_{y2}}{p}\right) l_{fe} \tag{11}$$

where r_j is the outer radius of the stator, d_{y2} is the yoke thickness of the motor with a 2-pole configuration.

Yoke eddy current loss can be derived from (4) and (11)

$$P_{ey} = \frac{\pi p n^2}{112\alpha} k_r k_e B_y^2 d_{y2} l_{fe}\left(r_j - \frac{d_{y2}}{p}\right). \tag{12}$$

From (6) and (11), yoke hysteresis loss can be expressed as

$$P_{hy} = \frac{\pi np}{60} k_h B_y^{\beta} V_y = \frac{\pi^2 n}{15} k_h B_y^{\beta} d_{y2} l_{fe}\left(r_j - \frac{d_{y2}}{p}\right). \tag{13}$$

Therefore, yoke eddy current loss is proportional to the number of poles while yoke hysteresis loss remains roughly constant when the number of poles is changed.

Taking the 4-pole PM motor as an example, the iron losses are calculated and listed in Table III as functions of number of poles. The total number of slots is $S = 36$. The possible numbers of poles are 2, 4, 6, and 12 with number of slots per pole per phase of 6, 3, 2, and 1 respectively. In order to achieve desired operation speed, the operation frequency proportionally increases with the number of poles. It can be seen from Table III that the total iron losses of the motor approximately increase 24 Watts if the number of poles increases by two.

TABLE IV
THEORETIC TORQUE AS A FUNCTION OF THE NUMBER OF POLES

Number of poles	2	4	6	12
Developed torque (Nm)	18.9	26.5	29.1	31.6
Increase of torque (%)	-	40.2	9.6	8.6

Therefore, we can express the total iron losses $P_{\rm iron}$ as a function of the number of poles

$$P_{\rm iron} = 20 + 12p. \tag{14}$$

B. Torque and Number of Poles

The developed torque of a PM motor is [26]

$$T_q = 2\pi r^2 l_{fe} \alpha B_{1g} K_{1\delta} \quad ({\rm Nm}) \tag{15}$$

where $B_{1\rm g}$ and $K_{1\delta}$ are the rms values of the airgap flux and the linear current density on the stator inner periphery.

The linear current density can be expressed as a function of stator current [27]

$$K_{1\delta} = \frac{mWI_a}{\pi r} \quad ({\rm A/m}) \tag{16}$$

where W is the total number of turns for each phase, r is the inner radius of stator, and $I_{\rm a}$ is the rated stator current.

Therefore, motor torque is a function of rotor radius, airgap flux density and stator current. If the airgap flux density and stator current are assumed constant, then

$$T_q = k_T r \quad ({\rm Nm}) \tag{17}$$

where $k_{\rm T}$ is a constant

$$k_T = 2m\alpha W I_a B_{1g} l_{fe}. \tag{18}$$

Assuming that the height of slots is kept constant, then the inner radius of the stator can be expressed as a function of the number of poles

$$r = r_j - \frac{2d_{y2}}{p} - d_t \tag{19}$$

where $d_{\rm t}$ is the tooth height.

It can be seen from (19) that when p is small, the increase of r is significant as p is increased. Therefore, increasing the number of poles can increase torque.

For the 4-pole PM motor, the turns per phase is $W = 96$, airgap flux density is $B_{1\rm g} = 0.757{\rm T}$. Rated current is 16.7 A. Magnet coverage is 0.793. $k_{\rm T} = 439$. The torque is

$$T = k_T \left(r_j - \frac{2d_{y2}}{p} - d_t \right) = 439 \times \left(0.0778 - \frac{0.0696}{p} \right). \tag{20}$$

The quantified torque of this motor as a function of the number of poles is shown in Table IV.

It can be seen from Table VI that the torque increases by 40% and 10% respectively when the number of poles increases from 2 to 4 and from 4 to 6 respectively, while the torque only increases 8.6% when the number of poles increases from 6 to 12. Since the losses in the frame also increase as the number of poles is increased, further increase of torque is limited by the thermal considerations of the design.

TABLE V
DEVELOPED TORQUE AND CALCULATED EFFICIENCY AS A FUNCTION OF THE NUMBER OF POLES AT 1800 rpm

Number of poles	2	4	6	12
Actual torque (Nm)	18.9	26.5	29.1	31.6
Efficiency (%)	89.0	91.5	91.8	91.4

C. Optimal Number of Poles

Although using larger number of poles can increase the motor torque, the increase of torque is minimal when the number of poles reaches a certain limit. The permissible heat in the frame further limits the increase of number of poles. By choosing proper number of poles, the motor efficiency can be optimized. The motor efficiency is

$$\eta = \frac{P_2}{(P_2 + P_{fw} + P_{cu} + P_{iron})} \tag{21}$$

where P_2 is the output power of the machine, $P_{\rm fw}$ is the windage and friction loss, and $P_{\rm cu}$ is the stator copper loss.

Output power P_2 and iron loss $P_{\rm iron}$ are functions of number of poles p, friction loss $P_{\rm fw}$ can be assumed constant for a given speed. The optimal efficiency and number of poles can be found by solving

$$\frac{d\eta}{dp} = 0, \quad p = 2, 4, 6, 8 \cdots\cdots. \tag{22}$$

For the above example, assuming that the variation of copper loss is minimal, the combined copper, stray loss, friction and windage losses are 398 W. The approximated efficiency can be expressed as

$$\eta = \frac{6438 - \frac{5759}{p}}{\left(6438 - \frac{5759}{p}\right) + 398 + (20 + 12p)}. \tag{23}$$

The calculated torque and efficiency of the motor are listed in Table V. It can be seen from Table V that, amongst all possible choices for number of poles, 2-pole design has the least torque and lowest efficiency. The 4-pole, 6-pole and 12-pole designs have similar efficiency. Since the total losses of the 6-pole and 12-pole configuration may exceed the maximum dissipation capacity of the frame, the experimental PM motor was constructed with the 4-pole configuration. This 4-pole configuration is also the simplest to construct among the choices with optimized efficiency.

By using the 4-pole configuration it was also made possible to use the existing stator winding of the induction machine.

The optimum choices for the number of poles are different for different applications. It requires the balance of material usage, achieved maximal torque and efficiency, manufacturing cost and permissible heat dissipation of the frame. In small machines, the maximum number of slots limits the number of poles, which is limited by the minimum practical width of the stator teeth

TABLE VI
A COMPARISON OF MEASURED AND PREDICTED NO-LOAD IRON LOSSES OF THE EXPERIMENTAL MOTOR (WATTS)

Speed (RPM)	300	600	900	1200	1500	1800
Calculated	6.5	15.0	25.5	37.9	52.3	68.7
Measured	4.2	11.9	22.8	36.3	52.6	71.6

TABLE VII
MEASURED LOSSES AND EFFICIENCY OF THE EXPERIMENTAL PM MOTOR COMPARED TO THE INDUCTION MOTOR USING THE SAME FRAME

	PM motor	Induction motor
Rated power (kW)	5.0	3.7
Speed (RPM)	1800	1742
Rated line voltage (V)	208	208
Rated current (A)	16.7	16.7
Stator copper loss (W)	285 (1)	354(2)
Windage and friction loss (W)	41	41
Rotor loss (W)	0	145(3)
Iron loss + Stray load loss (W)	144 (4)	449(4)
Total losses (W)	470	989
Efficiency (%)	91.4	78.9
Power factor	0.91	0.78

In Table VII: (1) Stator copper loss of the PM motor was calculated using actual measured resistance (0.34 Ω) at load testing; (2) Stator copper loss of the induction motor was calculated using resistance (0.4228 Ω) at 130° C; (3) Rotor loss was calculated using rotor slip and rated power; (4) Iron loss and stray load loss were derived from the total losses.

and slots. Usually the best choices are four, six and eight poles among all the possibilities for a PM motor design.

VII. EXPERIMENTAL WORK

The experimental PM motor was constructed using the original frame of the induction motor mentioned in Section III. The optimum number of poles was determined to be 4 using equations given in Section VI. This choice of number of poles allows the use of the stator winding of the original induction motor. There were 36 slots on the stator. The number of slots, being 3 per pole-phase is, satisfies the cogging torque requirement described in Section V. The magnets were beveled and parallel magnetized.

The no-load iron losses of the experimental motor were measured using the procedure described in [23]. Table VI gives a comparison of the total calculated no-load iron losses of the experimental PM motor with measured no-load iron losses. As it can be seen from Table VI, the measured iron losses are in accordance with the calculated iron losses.

The overall losses and efficiency of the PM motor were measured using direct input/output method. The input to the stator and the shaft torque was measured at rated speed. The total iron loss under load condition, including stray load loss, is obtained by subtracting the total loss by no-load iron loss, windage and friction loss, and stator copper loss. The loss components are compared to those of the induction machine [28] as shown in Table VII. Both efficiency and power factor of the PM motor are higher than the induction motor due to reduction of total losses (including the rotor slip loss). It also is worth to note that we were able to run the PM motor at 5 kW despite the fact that the same frame, core and stator winding were used for both the induction and the PM synchronous machines. The increase of power output of the PM motor is mainly due to the decrease of the total losses and the increase of power factor of the PM motor.

The agreement between measurements and the calculations confirm that the approaches used in this paper are generally valid. Although only one configuration was built and tested, validity of the analysis method suggests that the proposed loss minimization approaches do stand. It is desirable though, that in the near future, a few configurations be built and tested to compare the iron losses for optimized design.

VIII. CONCLUSION

This paper presents a set of effective approaches to minimize the iron losses of surface-mounted PM synchronous machines. It was shown that the torque and efficiency of the PM motor can be optimized through the proper design of magnets and slots, and through the choice of number of poles.

The analyses were based on both time-stepped FEM and a simplified iron loss model. The conclusions were verified by the measurements on the experimental motor. The suggested approaches are directly applicable to the optimization of PM synchronous motors.

REFERENCES

[1] "Opportunities for Energy Savings in the Residential and Commercial Sectors With High-Efficiency Electric Motors," Final Rep., Arthur D. Little, Inc., 1999.
[2] H. E. Jordan, *Energy-Efficient Electrical Motors and Their Applications*. New York: Plenum, 1994.
[3] J. C. Andreas, *Energy-Efficient Electrical Motors*. New York: Marcel Dekker, 1992.
[4] K. H. J. Buschow, New permanent magnet materials, in Mat. Sci. Rep., vol. 1, Sep. 1986.
[5] S. Nadel, *Energy Efficient Motor Systems' Handbook*: America Council for an Energy Efficient Economy, 1991.
[6] N. Urasaki, T. Senjyu, and K. Uezato, "Investigation of influences of various losses on electromagnetic torque for surface-mounted permanent magnet synchronous motors," *IEEE Trans. Power Electron.*, vol. 18, no. 1, pp. 131–139, Jan. 2003.
[7] A. A. Arkadan, R. Vyas, J. G. Vaidya, and M. J. Shah, "Effect of toothless stator design and core and stator conductors eddy current losses in permanent magnet generators," *IEEE Trans. Energy Convers.*, vol. 7, no. 1, pp. 231–237, Mar. 1992.
[8] K. Sitapati and R. Krishnan, "Performance comparisons of radial and axial field, permanent-magnet, brushless machines," *IEEE Trans. Ind. Appl.*, vol. 37, no. 5, pp. 1219–1226, Sep./Oct. 2001.
[9] K. Yamazaki, "Torque and efficiency calculation of an interior permanent magnet motor considering harmonic iron losses of both the stator and rotor," *IEEE Trans. Magn.*, vol. 39, no. 3, pp. 1460–1463, May 2003.
[10] F. Deng, "An improved iron loss estimation for permanent magnet brushless machines," *IEEE Trans. Energy Convers.*, vol. 14, no. 4, pp. 1391–1395, Dec. 1999.
[11] K. Atallah, Z. Q. Zhu, and D. Howe, "An improved method for predicting iron losses in brushless permanent magnet DC drives," *IEEE Trans. Magn.*, vol. 28, no. 5, pp. 2997–2999, Sep. 1992.
[12] N. Urasaki, T. Senjyu, and K. Uezato, "A novel calculation method for iron loss resistance suitable in modeling permanent-magnet synchronous motors," *IEEE Trans. Energy Convers.*, vol. 18, no. 1, pp. 41–47, Mar. 2003.
[13] H. Shimoji, M. Enokizono, and T. Todaka, "Iron loss and magnetic fields analysis of permanent magnet motors by improved finite element method with E&S model," *IEEE Trans. Magn.*, vol. 37, no. 5, pp. 3526–3529, Sep. 2001.
[14] Z. J. Liu, C. Bi, and T. S. Low, "Analysis of iron loss in hard disk drive spindle motors," *IEEE Trans. Magn.*, vol. 33, no. 5, pp. 4089–4091, Sep. 1997.

[15] B. Stumberger, A. Hamler, and B. Hribernik, "Analysis of iron loss in interior permanent magnet synchronous motor over a wide-speed range of constant output power operation," *IEEE Trans. Magn.*, vol. 36, no. 4, pp. 1846–1849, Jul. 2000.
[16] F. Fernandez-Bernal, A. Garcia-Cerrada, and R. Faure, "Determination of parameters in interior permanent-magnet synchronous motors with iron losses without torque measurement," *IEEE Trans. Ind. Appl.*, vol. 37, no. 5, pp. 1265–1272, Sep. 2001.
[17] Z. Q. Zhu, Y. S. Chen, and D. Howe, "Iron loss in permanent-magnet brushless AC machines under maximum torque per ampere and flux weakening control," *IEEE Trans. Magn.*, vol. 38, no. 5, pp. 3285–3287, Sep. 2002.
[18] P. J. Hor, Z. Q. Zhu, and D. Howe, "Eddy current loss in a moving-coil tubular permanent magnet motor," *IEEE Trans. Magn.*, vol. 35, no. 5, pp. 3601–3603, Sep. 1999.
[19] S. Morimoto, Y. Tong, Y. Takeda, and T. Hirasa, "Loss minimization control of permanent magnet synchronous motor drives," *IEEE Trans. Ind. Electron.*, vol. 41, no. 5, pp. 511–517, Oct. 1994.
[20] G. Bertotti, A. A. Boglietti, and M. Chiampi *et al.*, "An improved estimation of iron losses in rotation electrical machines," *IEEE Trans. Magn.*, vol. 27, no. 6, pp. 5007–5009, Nov. 1991.
[21] G. R. Slemon and X. Liu, "Core losses in permanent magnet motors," *IEEE Trans. Magn.*, vol. 26, no. 5, pp. 1653–1655, Sep. 1990.
[22] G. R. Slemon, *Electrical Machines and Drives*. Reading, MA: Addison-Wesley, 1992.
[23] C. Mi, G. R. Slemon, and R. Bonert, "Modeling of iron losses of permanent-magnet synchronous motors," *IEEE Trans. Ind. Appl.*, vol. 39, no. 3, pp. 734–742, May 2003.
[24] T. Z. Li and G. R. Slemon, "Reduction of cogging torque in permanent magnet motors," *IEEE Trans. Magn.*, vol. 24, no. 6, pp. 2901–2903, Nov. 1988.
[25] G. R. Slemon, "On the design of permanent magnet synchronous motors," *IEEE Trans. Ind. Appl.*, vol. 30, no. 1, pp. 134–140, Jan./Feb. 1994.
[26] ——, "Design of permanent magnet AC motors for variable speed drives," in *Performance and Design of Permanent Magnet AC Motor Drives*. New York: IEEE Press, 1991, ch. 3.
[27] S. Chen, *Electrical Machine Design, in Chinese*. Beijing, China: Mechanical Press, 1993.
[28] T. Sebastian, "Steady state performance of variable speed permanent magnet synchronous motors," Ph.D. dissertation, Dept. Elect. Comput. Eng., Univ. Toronto, Toronto, ON, Canada, Oct. 1986.

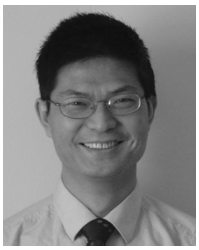

Chunting Chris Mi (S'00–A'01–M'01–SM'03) received the B.S.E.E. and M.S.E.E. degrees in electrical engineering from Northwestern Polytechnical University, Xi'an, China, and the Ph.D degree in electrical engineering from the University of Toronto, Toronto, ON, Canada.

Currently, he is an Assistant Professor with the University of Michigan, Dearborn, responsible for teaching power electronics, electric vehicles, electric machines, and drives. From 2000 to 2001, he was an Electrical Engineer with General Electric Canada Inc., Peterborough, ON. He was responsible for designing and developing large electric motors and generators up to 30 MW. He began his career at the Rare-Earth Permanent Magnet Machine Institute of Northwestern Polytechnical University, Xi'an, China. He joined Xi'an Petroleum Institute, Xi'an, China, as an Associate Professor and Associate Chair of the Department of Automation. He was a Visiting Scientist at the University of Toronto, Toronto, ON, Canada, from 1996 to 1997. He recently developed a Power Electronics and Electrical Drives Laboratory at the University of Michigan, Dearborn. His research interests include electric drives and power electronics, induction, brushless, and PM synchronous machines, renewable energy systems, and electrical and hybrid vehicle powertrain design and modeling.

Dr. Mi is the Chair of the Power and Industrial Electronics Chapter of the IEEE Southeast Michigan Section.

Gordon R. Slemon (S'46–A'48–M'48–SM'55–F'75–LF'90) received the B.A.Sc. and M.A.Sc. degrees from the University of Toronto, Toronto, ON, Canada, the D.I.C. from the Imperial College of Science and Technology, London, U.K., and the Ph.D. and D.Sc. degrees from the University of London, London, U.K.

Currently, he is a Consultant to industry and government as well as continuing his research specialty of electric machines and drives. Following employment with Ontario Hydro and Atomic Energy of Canada, he taught at Nova Scotia Technical College prior to his appointment to the staff of the Department of Electrical Engineering at the University of Toronto in 1955. He served as Head of its Electrical Engineering Department from 1966 to 1976, and as Dean of its Faculty of Applied Science and Engineering from 1979 to 1986. He is also Professor Emeritus in Electrical and Computer Engineering at the University of Toronto. He is the author or coauthor of five textbooks and 170 technical papers.

Dr. Slemon is an Officer of the Order of Canada and a Fellow of the Institution of Electrical Engineers, U.K., the Engineering Institute of Canada, and the Canadian Academy of Engineering. In 1990, he received the IEEE Nikola Tesla Award and IEEE Gold Medal.

Richard Bonert (M'81) received the Dipl.-Ing. and Doctorate degrees in electrical engineering from the University of Karlsruhe, Karlsruhe, Germany, in 1969 and 1977, respectively.

Currently, he is a Professor in the Power Systems and Devices Research Group at the University of Toronto, Toronto, ON, Canada. He joined Brown Boveri, Manheim, Germany, in 1969 as a Project Engineer, where he was engaged in designing electrical equipment for rolling mills, in particular, controlled electric drives. In 1971, he joined the Elektrotechnisches Institut, University of Karlsruhe, as a Research Associate and Chief Engineer for the experimental facilities. His area of research and teaching was power-semiconductor-controlled drives. After receiving a Research Fellowship, he worked in the Department of Electrical Engineering, University of Toronto, in 1978–1979. His main interests are power-semiconductor-controlled electric drives and power-electronics circuits, and the application of programmable electronics circuits in this field. He has a strong interest in laboratories for power engineering to support graduate research and education in engineering.